

Nanofiltration-Enhanced Solvent Extraction of Scandium from TiO₂ Acid WasteSebastian Hedwig,[▽] Bengi Yagmurlu,[▽] Danyu Huang, Oliver von Arx, Carsten Dittrich, Edwin C. Constable, Bernd Friedrich, and Markus Lenz*Cite This: *ACS Sustainable Chem. Eng.* 2022, 10, 6063–6071

Read Online

ACCESS |



Metrics & More

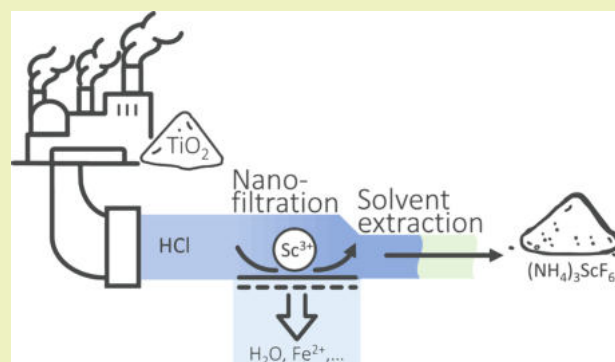


Article Recommendations



Supporting Information

ABSTRACT: Scandium is a critical raw material with a technological potential to reduce transportation costs and CO₂ emissions. However, global supply and market adoption are crucially impaired by the lack of high-grade Sc ores and recovery strategies. A tandem nanofiltration solvent extraction route is demonstrated to enable effective Sc recovery from real-world acid waste from the chloride TiO₂ production route. The process involving several filtration stages, solvent extraction, and precipitation was optimized, ultimately producing >97% pure (NH₄)₃ScF₆.



KEYWORDS: advanced membrane filtration, hydrometallurgy, element recovery, critical raw materials, waste valorization

INTRODUCTION

The intensifying climate crisis demands the transition of society to alternative technologies that can reduce anthropogenic greenhouse emissions to an environmentally acceptable level. Rare-earth element (REE) scandium (Sc) offers opportunities for “greening” the energy and transportation industries. For example, solid oxide fuel cells containing Sc can economically produce electricity from hydrogen and Sc is the most efficient dopant for aluminum alloys, allowing the production of ultralight car bodies.^{1,2} Minute amounts of Sc are sufficient for making aircraft Al alloys weldable and 3D printable, with up to 20% weight-saving for future aircraft construction.³

However, Sc has not been widely adopted by the industry due to limited market availability and astronomical prices (Sc₂O₃: 2200 USD kg^{−1} in 2021).⁴ Suppliers face a number of challenges with regard to Sc: reluctant customers, technologically demanding production processes, and shortages of high-quality Sc ores. Due to its (potential) economic importance, which is impeded by a pronounced supply risk, Sc has been classified as a critical raw material (CRM) by the European Commission since 2017.^{5,6} The European CRM initiative seeks for measures to remove supply bottlenecks for important commodities. One important strategy is to untap so far unused sources, such as industrial wastes. Although Sc rarely occurs naturally in concentrated ores, it is rather abundant in the Earth’s crust (Sc, 22 ppm; Pb, 14 ppm). Overall, Sc is present in hundreds of commercial minerals and can be found in waste streams of mineral industrial processes.^{7–9} White pigment

(TiO₂) has a global production volume of 8,000,000 t·a^{−10,11} with about half of the TiO₂ being produced by chloride route¹² in which TiO₂-rich ore is digested at high temperatures with elemental chlorine and coke. Volatile TiCl₄ is generated and can be condensed from the off-gases of the process. Afterward, TiCl₄ is converted to pure TiO₂ and Cl₂, the latter being recycled. Chlorides of accompanying metals enter the scrubbing water, which eventually turns into a semiconcentrated HCl slurry containing unreacted ore, coal particles, and numerous dissolved metals.^{13,14} Among these, Sc is in the hundred ppm range, making TiO₂ acid waste a promising Sc resource.⁵

Solvent extraction (SX) is the most commonly used technique to separate and concentrate Sc from aqueous solutions.^{7,15–20} The commonest extractants are organophosphorus compounds, such as di-(2-ethylhexyl)phosphoric acid (D2EHPA).^{7,15–19} Nevertheless, extraction of trace Sc from complex aqueous media remains technically challenging, requiring high aqueous to organic phase ratios, with the higher costs and emissions associated with large process volumes. In addition, coextraction of impurities (e.g., Fe, Ti, Zr, Th, U,

Received: February 21, 2022

Revised: April 14, 2022

Published: April 27, 2022



etc.) reduces the loading capacity and selectivity of the system and directly affects the final purity of the product.^{2,21–23} Therefore, strategies for preconcentration of Sc upstream to SX and reduction of impurities are urgently sought.

One possibility could involve membrane-based techniques such as nanofiltration (NF), which rely on other separation principles than SX.³ NF membranes bear pores of 0.2–2 nm, corresponding to a molecular weight cut-off (MWCO) of 200–1000 Da. Separation of solutes during NF is based on the size as well as electrostatic interactions in the case of dissolved ions. Typically, multivalent ions show high retention in NF, while monovalent species easily permeate. Recently, Remmen et al. demonstrated the potential of NF for Sc recovery from TiO₂ acid waste.³ However, only diluted acid waste was tested and downstream processing was not considered.

Therefore, our study investigated the process engineering needed for Sc recovery from TiO₂ waste, using NF combined with SX, with a view to real-world future implementation. NF was examined using commercial membranes under relevant operating conditions, such as high pressure and with undiluted acid waste. A variety of commercially available acid-resistant NF membranes was tested to account for differences between fabrications and manufacturers. Eventually, NF was used to produce a Sc concentrate from the acid waste.

Sc SX was examined for both the acid waste and the NF concentrate. In this context, the benefits and limitations of upstream NF prior to SX were investigated. Effects such as changes in coextraction, Sc yield, need for post-treatment, and plant dimensioning were considered, each being difficult to predict in advance. Ultimately, the overall process was evaluated in regard to implementation possibility for TiO₂ manufacturing via the chloride route.

MATERIALS AND METHODS

Chemicals and Materials. Acid waste was provided from a TiO₂ producer located in the Netherlands. All aqueous solutions were prepared using ultrapure water (>18 MΩ; Barnstead Smart2Pure water purification system, Thermo Fisher Scientific, Switzerland). For pH adjustment, NaOH solution (30 wt %) was used together with a pH meter (inoLab Multi 9310 IDS, WTW, Germany). Suspended solids were removed by microfiltration using (1) vacuum filtration in combination with glass fiber filters (0.4 μm, MN GF-5, Macherey-Nagel, Germany) or (2) decantation and gravity filtration with filtration bags (1 μm, Eurowater, Germany). Residual suspended particles were removed by ultrafiltration (MWCO 150 kDa, UP150, Microdyn-Nadir, Germany).

Analytical Methods. *QqQ-ICP-MS.* Samples were diluted with nitric acid (3%) using an autodilution system (SimpRep, Teledyne Cetac Technologies). Samples were analyzed using triple quadrupole inductively coupled plasma mass spectrometry (QqQ-ICP-MS) as previously described.⁵ The analysis was performed on an 8800 QqQ-ICP-MS system (Agilent, Basel, Switzerland) using general-purpose operational settings. Quantification was performed via multielement standards (0–50 ppb, seven points). To account for matrix effects, ¹⁰³Rh was used as the internal standard. To quantify ²³Na⁺, ⁵²Cr⁺, ⁵⁵Mn⁺, ⁵⁶Fe⁺, ⁶⁰Ni⁺, ⁶⁶Zn⁺, ⁸⁹Y⁺, ¹³⁷Ba⁺, ¹³⁹La⁺, ¹⁴⁰Ce⁺, ¹⁴¹Pr⁺, ¹⁴⁶Nd⁺, ¹⁴⁷Sm⁺, ¹⁵³Eu⁺, ¹⁵⁷Gd⁺, ¹⁵⁹Tb⁺, ¹⁶³Dy⁺, ¹⁶⁵Ho⁺, ¹⁶⁶Er⁺, ¹⁶⁹Tm⁺, ¹⁷²Yb⁺, ²⁰⁸Pb⁺, ²³²Th⁺, and ²³⁸U⁺, ICP-MS was operated in the single quad mode using helium as a collision gas, whereas ²⁴Mg⁺, ²⁷Al⁺, ³⁹K⁺, ⁴⁵Sc⁺, ⁴⁷Ti⁺, ⁵¹V⁺, and ⁹⁰Zr⁺ were measured in the triple quad mass-shift mode using O₂ as a reaction gas. ⁷Li⁺ concentration was determined using the no-gas single quad mode.

Dead-End NF. For dead-end NF, an HP4750 stirred cell (Sterlitech, scheme available in the SI) was used. Flat sheet membranes (Table S1, SI) were cut into circular shapes and

immersed for >20 h in ultrapure water. Afterward, the membranes were inserted into the cell with the active side (14.6 cm²) oriented toward the feed solution (100 mL per experiment). The cell was closed, and the pressure was adjusted to 35 bar under continuous stirring (300 rpm). Unless otherwise described, filtration was carried out until 30% permeate was recovered (determined by weight).

Cross-Flow Filtration. For cross-flow filtration (UF and NF), a modular filtration unit (MaxiMem, PS Prozesstechnik, Switzerland) was used (P&I diagram available in the SI). Experiments with flat sheet membranes (active area: 200 cm²) were conducted at a cross-flow flux of 5 L min^{−1} and a temperature of 25 °C. Spiral wound elements (1812 type: 1.8" diameter, 12" length, 31 mil spacer, 0.32 m² active area) were used at a cross-flow flux of 10 L min^{−1} and a temperature of 25 °C. Ultrafiltration (UF) was conducted isobarically at 10 bar under flat sheet conditions. Prior to use, NF membranes were compacted at 10 bar overnight using ultrapure water.

SX. Solvent extraction tests were conducted in a glass beaker with a phase ratio of 1 (50 mL:50 mL). Each organic phase was contacted with untreated acid waste and NF concentrate for 15 min to reach the equilibrium under mild stirring at room temperature. The selected organic phase was loaded with a phase ratio (volume of aqueous phase: volume of organic phase) of 7 for investigations on scrubbing and stripping behavior. For investigation of loading and scrubbing dependency on Fe valency in the NF concentrate, iron metal (1.5 g L^{−1}) was added to reduce any Fe³⁺ to Fe²⁺.

For scrubbing tests, HCl (37%, laboratory grade) was diluted with ultrapure water to the desired concentrations. Stripping solutions were prepared using reagent-grade NH₄F. Extractants (D2EHPA, Cyanex 923, N1923, and tri-*n*-butyl phosphate (TBP)) were diluted with dearomatized kerosene (Exxsol D80, ExxonMobile, Germany). Aqueous and re-extraction solutions of the organic phases were sampled for the efficiency calculations.

The distribution ratio and the selectivity of the organic extractants are calculated according to the following equation

$$D_x = \frac{C_x^{\text{org}}}{C_x^{\text{aq}}} \text{ and } \alpha_{x/y} = \frac{D_x}{D_y} \quad (1)$$

where D_x is the distribution coefficient of element x , C_x is the concentration of element x in the aqueous/organic phase, and α is the extraction selectivity.

RESULTS AND DISCUSSION

pH Adjustment/Preparation of NF Feed. The acidic waste from the European TiO₂ production site contained suspended solids (mainly overblown coke and unprocessed ore) and numerous elements in widely varying concentrations. Some of the elements present were known to be problematic for Sc recovery via SX (e.g., Ti, Zr) or potentially hazardous to health and safety (naturally occurring radioactive material, NORM).⁷ Ti can be retained in the solution or scrubbed out of the extractant during SX of the waste from the alternative sulfuric acid TiO₂ production process by adding H₂O₂ to facilitate formation of Ti peroxo sulfate complexes,¹⁶ although this is not possible in the chlorine process in which Ti must be removed before SX.

Excellent separation of Sc from Ti, Zr, and Th was achieved at pH 1–1.5 (Figure 1). Most of the Sc (82 ± 1% at pH 1; 68 ± 1% at pH 1.5) remained in the solution, while the other metals precipitated quantitatively (>99%). Adjusting the pH to 1.5 was considered as the best option, as the majority (69 ± 1%) of U also precipitated (Figure 1).

In general, Sc precipitation started at pH > 1 and was completed at pH 2.5. For Ti, Zr, and Th a steep drop in solubility was observed between pH 0.5 and 1 (Figure 1). Further, U precipitated slightly faster than Sc, starting at pH < 1 and being >95% precipitated by pH 2 (Figure 1). In contrast,

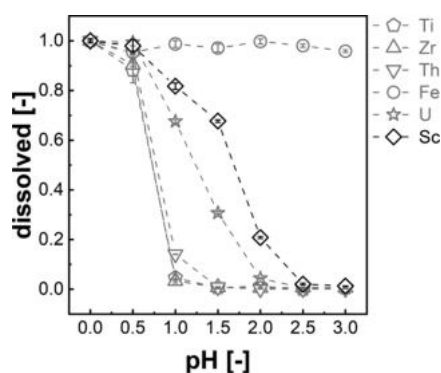


Figure 1. Dissolved elements in the acid waste during neutralization with NaOH.

Fe remained completely dissolved within the range of pH 0–3 (Figure 1). The high solubility of Fe indicated the predominant presence of ferrous iron instead of ferric iron,²⁴ as the latter precipitates at pH ≥ 3 .

After pH adjustment, element concentrations in the supernatant were monitored over two weeks. Concentrations were mostly stable over time at different pH values, except near the inflection point of precipitation, where no plateau was reached even after two weeks. There, concentrations increased over time, presumably as a correction of overprecipitation due to local supersaturation.²⁵ At a pH of 1.5, an equilibration time of 48 hours after NaOH addition was found sufficient.

During S/L separation of the slurry (pH = 1.5), the precipitated hydroxides and oxides were only filtered with difficulty. With filter bags (1 μm sieve size), the filtrate was still turbid, while 0.4 μm filters clogged rapidly. The best procedure involved sedimentation of the precipitate (≈ 48 h) followed by decantation and bag filtration to give a clear solution. The solid fraction (approx. 32% v/v) was a moist gel.

Following microfiltration, residual particles were removed by UF to prevent scaling in subsequent processing. The microfiltrate was easily filterable, with losses determined by the dead volume of the filtration unit (≈ 200 mL). The UF permeate, obtained after the pretreatment, is subsequently referred to as NF feed.

Only few studies on the precipitation behavior of Sc and other elements contained in the acid waste of the TiO_2 chloride route have been reported. Most recently, Remmen et al. described precipitation trends at a pH of 1.5 for different

elements in the waste.³ The precipitation trends at pH 1.5 presented here conform with those previously reported.³ However, in our system, more precipitation was observed (Sc, $\sim 30\%$; Th, $>99\%$; and U, $\sim 70\%$ (here) vs Sc, $\sim 20\%$; Th, 80%; U, 40% (Remmen et al.)).³ We assume that this arises from the removal of microparticles by UF. Otherwise, pH values of incipient precipitation reported were extremely low for various elements compared to other literature.^{26–29} Precipitation of Th and U is reported to occur between pH 5 and 7 from chloride media (1–2 for Th from sulfate media).²⁶ Sc reportedly precipitated at pH ≥ 3 in HCl.²⁹ Presumably, the high concentrations of Ti and Zr, whose hydroxides are known to be barely soluble even at a pH of <2 , result in coprecipitation.²⁷

Overall, the results show that the precipitation of elements in complex real solutions can deviate greatly from findings in model solutions. Although precipitation rates and solubility products are known for the pure compounds, effects such as sorption/coprecipitation and kinetic limitations in complex mixtures make ab initio predictions of behavior very difficult, making extensive testing inevitable when developing processes based on secondary resources.

NF-Membrane Screening. Six potential NF-membrane candidates were compared in terms of (1) permeate flux (Figure 2A), (2) element retention (mainly R_{Sc} and R_{Fe} ; Figure 2B), and (3) Sc selectivity (expressed through R_{Sc} divided by R_{Fe} ; Figure 2C) during filtration of the NF feed. The membrane showing the best performance of high permeate flux, and high R_{Sc} , while being permeable for competing elements, was A3014, with a permeate flux of $6.7 \pm 0.8 \text{ Lm}^{-2} \text{ h}^{-1}$, a R_{Sc} of 0.81 ± 0.03 , and a Sc over Fe selectivity of 1.9 ± 0.4 .

The tested membranes had permeate fluxes ranging from 0.25 to $35 \text{ Lm}^{-2} \text{ h}^{-1}$, in the order A3012 < KH < DK < NP030 < A3014 < MPF36 (Figure 2A), largely consistent with the MWCO reported by the manufacturers (Table S1, SI), with tighter membranes (A3012, DK, KH) showing lower fluxes.

Sc retentions were between 0.49 and 0.95, in the order NP030 < MPF36 < KH < A3014 < DK < A3012 (Figure 2B). For Fe, retentions in the range of 0.32–0.90 were observed, following the order MPF36 \approx NP030 < AMS3014 < KH < DK < A3012 (Figure 2B). At last, in terms of Sc over Fe selectivity, a range of 1 (no selectivity) to 2 was found, following the order A3012 < DK < KH < NP030 < A3014 < MPF36 (Figure 2C).

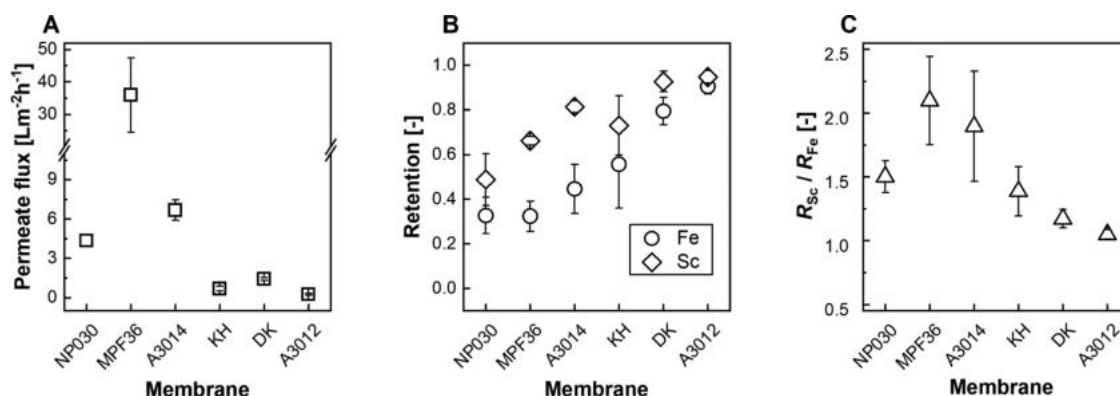


Figure 2. Permeate flux (A), element retention (B), and quotient of Sc over Fe retention (C) (dead-end filtration at 35 bar and 30% permeate recovery).

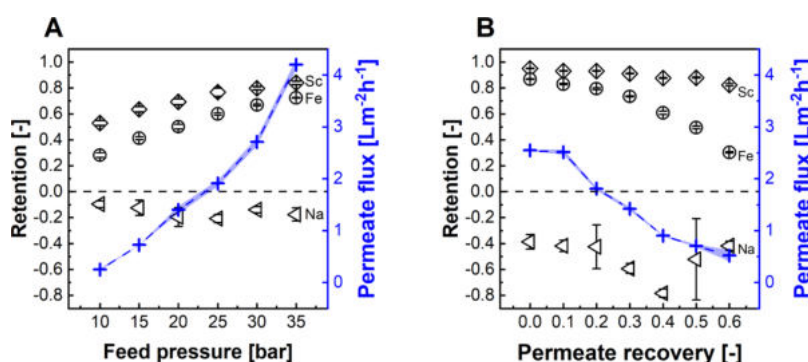


Figure 3. Element retention and permeate flux against the feed pressure at 0% permeate recovery (A) and element retention and permeate flux against the permeate recovery rate at 35 bar (B).

Table 1. Volumes and Elemental Concentrations for Different Streams during the Production of the NF Concentrate and Elemental NF Yields and Concentration Ratios for Comparison of the NF Concentrate with NF Feed and Initial Waste

| | initial waste | microfiltrate | NF feed | NF concentrate | NF yield | concentrate/initial waste | concentrate/NF feed |
|--------------------------|---------------|---------------|--------------|----------------|-------------|---------------------------|---------------------|
| volume [L] | 3.2 | 2.2 | 2.0 | 0.8 | | 0.24 | 0.37 |
| Sc [mg L ⁻¹] | 41.1 ± 0.1 | 33.3 ± 0.5 | 28.9 ± 0.5 | 61 ± 2 | 0.84 ± 0.03 | 1.5 | 2.1 |
| Ti [mg L ⁻¹] | 4540 ± 10 | 28.5 ± 0.6 | 5.1 ± 0.2 | 8.1 ± 0.4 | 0.64 ± 0.04 | 0.002 | 1.6 |
| Zr [mg L ⁻¹] | 1170 ± 20 | 8.0 ± 0.3 | 0.12 ± 0.03 | 0.19 ± 0.02 | 0.63 ± 0.17 | 0.0002 | 1.6 |
| Al [mg L ⁻¹] | 1730 ± 10 | 1611 ± 30 | 1430 ± 11 | 2950 ± 70 | 0.83 ± 0.02 | 1.7 | 2.1 |
| Fe [mg L ⁻¹] | 17 600 ± 200 | 17 100 ± 100 | 15 800 ± 200 | 23 100 ± 600 | 0.58 ± 0.02 | 1.3 | 1.5 |
| Th [mg L ⁻¹] | 79 ± 1 | 5.8 ± 0.2 | 2.9 ± 0.1 | 5.4 ± 0.01 | 0.74 ± 0.03 | 0.07 | 1.9 |
| U [mg L ⁻¹] | 13.9 ± 0.2 | 0.29 ± 0.01 | 0.09 ± 0.01 | 0.10 ± 0.01 | 0.44 ± 0.07 | 0.006 | 0.9 |
| V [mg L ⁻¹] | 1070 ± 20 | 930 ± 30 | 840 ± 20 | 1340 ± 40 | 0.64 ± 0.02 | 1.3 | 1.6 |
| Na [mg L ⁻¹] | 150 ± 30 | 29 000 ± 1000 | 26 000 ± 300 | 15 000 ± 400 | 0.28 ± 0.01 | 100 | 0.6 |
| Mn [mg L ⁻¹] | 4600 ± 200 | 4600 ± 100 | 4400 ± 100 | 5500 ± 200 | 0.5 ± 0.02 | 1.2 | 1.3 |

While the MWCOs were found to be helpful in explaining the trends, there were also exceptions, e.g., the loosest membrane (MPF36, MWCO 1000 Da) showed the highest flux but not the lowest Sc retention. Instead, NP030 (MWCO 500 Da) retained the least Sc, while Fe retention appeared similar to MPF36. NP030 showed also a lower flux than A3014 (MWCO 400 Da), although being potentially looser.

Low element retention has already been reported for NP030. Kose Mutlu et al. tested NP030 and the DK for REE recovery from fly ash leachate at low pH.³⁰ REE retentions were some eight times lower for NP030 in comparison to DK,³⁰ and pH-dependent zeta-potential measurements revealed considerably higher positive surface charges for DK than those for polyether sulfone membrane NP030.³⁰ Hence, a potential Donnan rejection mechanism was less pronounced and element retention was lower for NP030 than that for other membranes.

For NF-based Sc recovery, only MPF36 and A3014 were suitable, as both exhibited good Sc over Fe selectivity and sufficient permeate fluxes. Of the two potential candidates, A3014 was selected for further process development, as a high R_{Sc} , crucial for low Sc losses, was considered more important than high permeate flux. However, MPF36 may represent an interesting choice, when yields are less important than filtration time and operation costs.

Remmen et al. developed layer-by-layer (LbL)-assembled NF membranes, which showed a R_{Sc} of up to 0.60 compared to a R_{Fe} of >0.05 and high permeate flux (up to 28 Lm⁻² h⁻¹) at just 5 bar.³ Aside from NP030, all commercial membranes had not only higher R_{Sc} but also higher R_{Fe} values. Therefore, more Sc could be recovered with commercial membranes, but at lower selectivity reaching maximally two times higher R_{Sc} (0.66

and 0.81) than R_{Fe} (0.32 and 0.44) for MPF36 and A3014, respectively. Further, the permeate fluxes were considerably lower compared to LbL membranes: 35 bar pressure was necessary for MPF36 to reach 36 Lm⁻² h⁻¹, while the second fastest membrane (A3014) reached only ~7 Lm⁻² h⁻¹. However, the test conditions differed to those of Remmen et al., where the acid waste was diluted (1:5).³ With the higher initial concentration of the feed, a correspondingly higher osmotic pressure had to be overcome and a higher operational pressure was inevitable.

NF Process for Acid Waste Concentration. In the cross-flow filtration mode with A3014, 35 bar (maximum feed pressure) was optimal in regard to permeate flux (4.2 ± 0.1 Lm⁻² h⁻¹) and R_{Sc} (0.84 ± 0.01). For Sc selectivity, 1.2 times higher R_{Sc} than R_{Fe} was observed.

Increasing the feed pressure led to an almost linear increase of the permeate flux from 0.25 ± 0.02 Lm⁻² h⁻¹ (10 bar) to 4.2 ± 0.1 Lm⁻² h⁻¹ (35 bar; Figure 3A). At the same time, R_{Sc} improved from 0.53 ± 0.02 (10 bar) to 0.84 ± 0.01 (35 bar; Figure 3A). In comparison, R_{Fe} started at 0.28 ± 0.02 (10 bar) and increased to 0.72 ± 0.01 (35 bar). Since R_{Fe} increased faster than R_{Sc} , the selectivity of Sc over Fe decreased from 1.9 (10 bar) to 1.2 (35 bar). In comparison to Sc and Fe, monovalent cations, such as Na⁺, were well permeable, indicated by negative retentions throughout the experiments (Figure 3A). Element retentions increased with higher feed pressure due to the subordinate role of diffusive salt transport with a simultaneous increase in water permeation.³¹

With regard to R_{Fe} , a discrepancy between cross-flow (0.72) and dead-end (0.44) filtration was observed, while R_{Sc} was similar (~0.8) in both cases. Therefore, Sc over Fe selectivity was lower during cross-flow tests. This is probably due to

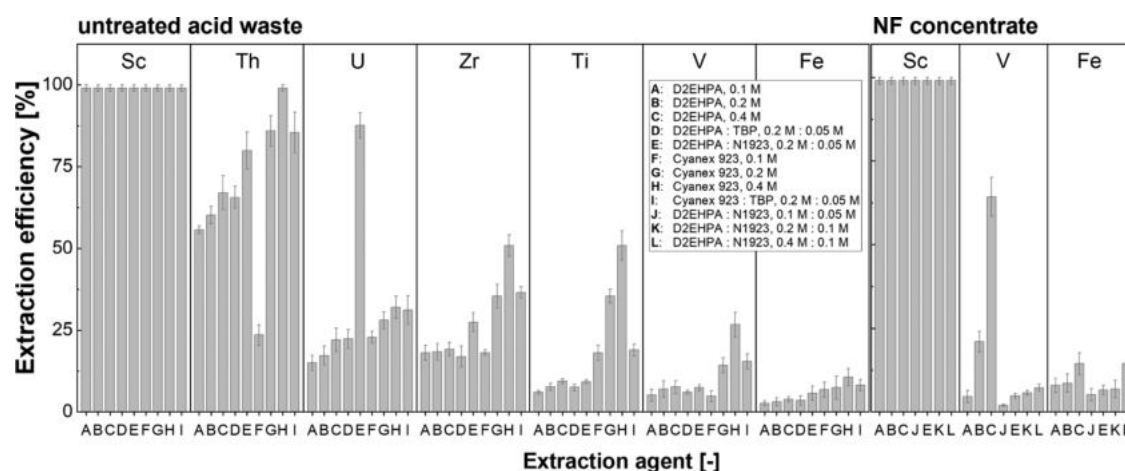


Figure 4. Organic screening for the optimization of the loading behavior both from untreated acid waste and NF concentrate (impurities with <10 ppm concentration are not included).

better compaction when using the cross-flow setup, explaining the higher retentions but also lower permeate flow in these tests.³² On the other hand, higher concentration polarization during dead-end filtration conjunct to stronger electrostatic repulsion for Sc^{3+} than that for Fe^{2+} might have led to the deterioration of R_{Fe} while being less important for R_{Sc} .³

In terms of energy consumption, maintaining the same cross-flow rate of 10 L min^{-1} at 35 bar required about 2.5 times more energy than that at 10 bar.³³ However, the permeate flow at 35 bar increased, in comparison, 17 times, shortening the operation time and compensating for the higher energy consumption at elevated pump loads. Therefore, in this case, concentrating can be considered more energy efficient at higher pressures.

Ultimately, from the 2.0 L NF feed, 0.8 L NF concentrate was produced. Overall, $84 \pm 3\%$ of Sc and $58 \pm 2\%$ of Fe remained in the solution (Table 1). The permeate recovery was stopped at around 60% due to a low permeate flux ($0.5 \text{ L m}^{-2} \text{ h}^{-1}$), a decreased R_{Sc} (0.12), and a low residual concentrate volume, being insufficient to maintain a cross-flow rate of 10 L min^{-1} .

The permeate flux decreased gradually from 2.5 ± 0.1 to $0.5 \pm 0.1 \text{ L m}^{-2} \text{ h}^{-1}$ (Figure 3B). In terms of element retentions, higher values were found than in the previous experiments. The R_{Sc} decreased from 0.95 ± 0.01 to 0.82 ± 0.01 and Fe became notably more permeable with increasing concentration, with R_{Fe} starting at 0.87 ± 0.01 and decreasing to 0.30 ± 0.01 at 60% permeate recovery. Therefore, the Sc over Fe selectivity improved from 1.1 to 2.7. Representative of monovalent ions, Na^+ , showed very high permeability throughout the experiment, permeating against its concentration gradient ($R_{\text{Na}} < -0.3$).

During concentration, permeate fluxes and element retentions decreased due to the osmotic pressure increase, as reported before.³ Interestingly, Sc retention was less affected than, e.g., Fe retention. It is assumed that this was caused by concentration polarization, being proportional to the element feed concentration and becoming even more prevalent as filtration progressed and concentrations increased.³⁴ Permeability, however, is expected to be lower for Sc^{3+} than that for Fe^{2+} due to the stronger Donnan exclusion. Hence, NF became more selective for Sc with the ongoing progress of the operation.

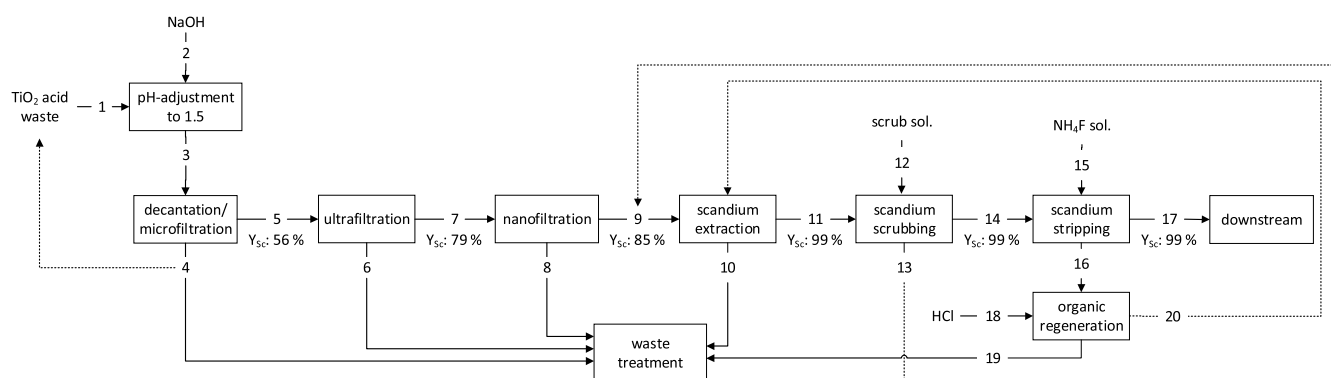
Solvent Extraction Behavior. Although various studies on the sulfate TiO_2 production route have been reported,^{16,17,35} limited information is available for SX processes on chlorine TiO_2 production waste. D2EHPA, Cyanex 923, and synergistic mixtures of these organics worked best to recover Sc selectively from complex solutions in the sulfate process. Therefore, these extractants were tested with various concentrations in D80 kerosene to observe the selectivity, phase separation behavior, and the coextraction levels of the impurities from untreated acid waste and NF concentrate (Figure 4).

All extractants performed similarly in Sc extraction, lowering the Sc concentration to <1 ppm after extraction in all tests with untreated acid waste (Figure 4). Increasing the D2EHPA concentration did not significantly increase the coextraction of impurities. While Ti, Zr, V, and Fe coextraction remained stable (Figure 4), extraction of radionuclides increased from 55 to 67% and 15 to 22% for Th and U, respectively. Unlike D2EHPA, increasing the Cyanex 923 concentration (to 0.4 mol L^{-1}) resulted in high coextraction of Th (> 99%), Ti (~50%), Zr (~50%), V (30%), and Fe (10%). No synergistic effect of TBP with these extractants was observed. Coextraction generally increased with the synergistic addition of N1923 to D2EHPA, reaching 85% for Th and 31% for U. Increased NORM extraction was expected, as amines are widely used in commercial solvent extraction of radioactive elements.³⁶ Even though promising extraction efficiencies were found, the phase separation was problematic in all cases due to high transition-metal loading.^{37–39} Formation of an inseparable phase occurred in all extraction trials with slow separation behavior, predicting a high loss of the organic phase and processing problems in a larger-scale continuous operation.

Extraction tests with the NF concentrate were carried out using the most promising extractants, D2EHPA and the synergistic D2EHPA–N1923 couple. Similar to the untreated acid waste, Sc was completely extracted when using the NF concentrate. However, high coextraction was found with D2EHPA as the extractant. This was especially pronounced for higher D2EHPA concentrations, reaching 65% for V and 14% for Fe at 0.4 mol L^{-1} D2EHPA (Figure 4). It was previously reported that addition of N1923 can substantially improve Sc selectivity.^{17,40,41} Here, addition of 0.05 mol L^{-1} efficiently suppressed V coextraction and slightly decreased Fe loading (Figure 4). Sc selectivity over other elements increased

Table 2. Compositions and Flows of Critical Elements through the Complete Solvent Extraction Process from the NF Concentrate to Strip Liquor

| | raffinate | loaded org. | scrubbed org. | scrubbed org. (stage 3) | stripped org. | strip liquor |
|--------------------------|--------------|-------------|---------------|-------------------------|---------------|--------------|
| Sc [mg L ⁻¹] | n.d. | 494 ± 7 | 492 ± 3 | 491 ± 4 | n.d. | 1468 ± 31 |
| Ti [mg L ⁻¹] | 2.7 ± 0.3 | 31.6 ± 1.8 | 9.8 ± 0.4 | 3.4 ± 0.08 | n.d. | 8.4 ± 1.2 |
| Zr [mg L ⁻¹] | n.d. | 2.4 ± 0.03 | 0.4 ± 0.02 | 0.2 ± 0.01 | 0.05 ± 0.02 | 0.5 ± 0.01 |
| Al [mg L ⁻¹] | 2912 ± 70 | 24.5 ± 0.8 | 7.4 ± 0.9 | 1.1 ± 0.06 | 0.3 ± 0.03 | 2.8 ± 0.05 |
| Fe [mg L ⁻¹] | 22 968 ± 600 | 676 ± 28 | 38.4 ± 2.2 | 3.2 ± 0.1 | n.d. | 9.9 ± 1.0 |
| Th [mg L ⁻¹] | 1.4 ± 0.1 | 22 ± 1.1 | 15.4 ± 0.7 | 8.6 ± 0.7 | 1.5 ± 0.05 | 23.4 ± 2.9 |
| U [mg L ⁻¹] | n.d. | 0.09 ± 0.01 | n.d. | n.d. | n.d. | n.d. |

**Figure 5.** Block flow diagram of the tandem NF-SX process for Sc recovery from TiO₂ acid waste.

during extraction with the synergistic D2EHPA–N1923 mixture (Table S2, SI). Phases separated rapidly during extraction of the NF concentrate, making the process viable for larger-scale operation.

Considering the loading capacity, selectivity toward Sc, and the phase separation, the best extractant option was identified as 0.2 mol·L⁻¹ D2EHPA with 0.05 mol·L⁻¹ N1923 in D80 kerosene.

Scrubbing. After SX with the selected organic and a phase ratio of 7, Sc was enriched considerably (0.49 g·L⁻¹). Of the major impurities present in the NF concentrate, Fe (6.3 g·L⁻¹) and Al (16 mg·L⁻¹) were found in the organic phase. The trace impurities in NF concentrate, Ti, Zr, and Th, were enriched in the organic phase after SX to 32, 25, and 20 mg·L⁻¹, respectively.

HCl was preferred as the scrubbing solution due to the strong interaction between Fe and Cl and avoiding unwanted complex formation from other anions.

No Sc was scrubbed out from the organic phase (Table S3, SI). With increasing HCl concentration, Ti, Zr, Th, and Al removal was only slightly improved, while the highest Fe removal (89%) was obtained with 4 mol·L⁻¹ HCl. Therefore, 4 mol·L⁻¹ HCl was selected for scrubbing after SX, removing aside from Fe also 72, 76, 20, and 56% of Ti, Zr, Th, and Al, respectively.

Although the majority of Fe in the NF concentrate was ferrous,²⁴ a fraction oxidized to ferric spontaneously. Presumably, the ferric portion caused high Fe coextraction, as the affinity of D2EHPA for Fe³⁺ is considerably higher than for Fe²⁺. To suppress Fe coextraction, iron metal was added to the NF concentrate, reducing Fe³⁺ to Fe²⁺ (eq 2).



Extraction from three post-treatments for the NF concentrate (original, reduced, and reduced and acidified) was compared in terms of Fe coextraction suppression capability.

Reduction of ferric iron resulted in a sharp decrease of the coextraction values; while 3.3 g·L⁻¹ Fe was coextracted with the original NF concentrate, only 0.36 g·L⁻¹ Fe after reduction and 0.17 g·L⁻¹ Fe after reduction and acidification were extracted. Thus, reduction and optionally acidification enable complete Fe scrubbing during SX, requiring only a few mixer–settler units.

Stripping. Although D2EHPA is a very effective extractant for Sc extraction, its strong bonding characteristics make Sc stripping from the organic phase challenging. Concentrated acids as well as strong alkali solutions have been used for stripping.⁴² However, even highly concentrated acids were relatively unsuccessfully, and concentrated NaOH solutions were used instead.⁴³ Nevertheless, other problems arise from stripping of D2EHPA with NaOH: (1) loss of organics due to solubility of Na-D2EHPA in aqueous solutions, (2) separation issues with the third phase formation owing to solubility variations of the extractant in kerosene, and (3) immediate precipitation of Sc(OH)₃ and clogging of the liquid flow in continuous operation.^{38,44,45}

Therefore, NH₄F was selected as the stripping agent due to stable and strong complexation forming (NH₄)₃ScF₆. Here, quantitative (>99%) Sc stripping was achieved (Table 2). The final product contained only traces of impurities, wherefore Sc accounted for ~97 wt % of the metals in the strip liquor (Table 2). Residual impurities could be removed via antisolvent crystallization, yielding pure (NH₄)₃ScF₆.⁴⁶ Calcination of this product gives easy access to ScF₃, which can be directly utilized in Al–Sc alloy production.⁴⁶ Therefore, high-temperature processing to convert Sc(OH)₃ into Sc₂O₃ or treatment with gas-phase HF to produce ScF₃ can be avoided.

Process Flow Scheme/Integration into the Chloride Route. The proposed Sc recovery process comprises seven

stages (Figure 5). From pH adjustment to NF, only sodium hydroxide, electrical power, and reusable filters/membranes were required. NaOH, although expensive compared to lime/limestone, was needed to avoid high multivalent cation concentrations (e.g., Ca^{2+}), which would be enriched during NF due to high retentions, increasing the osmotic pressure of the feed and opposing the feasibility of the filtration. However, in view of the overall process (i.e., Sc recovery conjunct to chloride-route TiO_2 production), NaOH might be available from upstream chlorine production via NaCl electrolysis, saving transportation costs.⁴⁷

In terms of Sc yields, the S/L separation (i.e., MF and UF) brought substantial losses (around 56%). Thus, despite the high yields (82%, four stages) following UF, the overall Sc yield was 36%. However, this could be mitigated by more efficient S/L of the hydroxide sludge, such as by the use of a filter press. Losses during lab-scale UF (stream 6) due to the dead volume of the filtration unit would become negligible on a larger scale. Alternatively, streams 4 and 6 could be redirected into the original acid waste. This would reduce the amount of Sc discharge. Neutralization followed by S/L separation is currently used for acid waste treatment after chlorine TiO_2 production. Hence, NF feed could be produced by minor adjustments to the current treatment conditions.

During NF, most of the Sc (85%) was preserved in the concentrate. The NF permeate (stream 8) is relatively diluted compared to the upstream media and could be reused as scrubbing water in the gas washer of the TiO_2 production process. This would contribute to a zero liquid discharge approach and would keep NF-related Sc losses in the system.

SX downstream to NF allowed for quantitative (99%) Sc recovery from the concentrate. Due to excellent phase separation, no organic should be in the raffinate (stream 10). This Sc-depleted solution could either be returned to the existing TiO_2 waste treatment process or could serve for further element recovery (e.g., V, Mn, other REE). The scrubbing effluent (stream 13) could be reused for acidification of the NF concentrate once Fe^0 was added (Figure S3, SI). Compared to the NF concentrate, the throughput of stream 13 was rather low. Hence, a combination of 13 and 9 would lead to negligible dilution but allow for waste mitigation and pH adjustment.

After Sc recovery via NF and SX, the Sc-depleted solutions could be returned to the existing waste treatment route.

CONCLUSIONS

A combination of NF and SX has been applied to recover Sc from acid waste, originating from chloride-route TiO_2 production. The major findings were as follows:

- pH adjustment to 1–1.5 preserved Sc dissolved and precipitated challenging impurities (Ti, Zr, Th, U)
- AMS Nanopro A-3014 provided the best tradeoff between permeate flux, Sc retention, and selectivity
- At the most effective pressure of 35 bar, 60% of the volume and various bulk impurities (such as ~40% Fe, V, Mn) were removed, while 85% of Sc remained in the concentrate
- A mixture of D2EHPA and N1923 was most selective in SX
- Upstream removal of Ti, Zr, Th, and U drastically increased Sc selectivity during SX

- NF prior to SX improved the phase separation and reduced the process volume
- Addition of Fe^0 suppressed Fe^{3+} coextraction and improved Fe scrubbing
- NH_4F was found to be a highly efficient stripping agent for Sc (purity >97%)
- Overall Sc recovery was 36% (six stages), which could be improved in the future by more efficient engineering of the MF and UF stages

The proposed process could be integrated into the waste disposal unit of a TiO_2 production plant without drastic plant changes and could be a step toward waste valorization and effective resource use, enabling the production of a CRM with promising future potential.

ASSOCIATED CONTENT

Supporting Information

The Supporting Information is available free of charge at <https://pubs.acs.org/doi/10.1021/acssuschemeng.2c01056>.

Descriptions and properties of the membranes, schemes of the used filtration units, comparison of Fe loading efficiencies, Sc selectivity over major impurities, and impurity scrubbing efficiencies from the loaded D2EHPA + N1923 (PDF)

AUTHOR INFORMATION

Corresponding Author

Markus Lenz – FHNW, Institute for Ecopreneurship, 4132 Muttentz, Switzerland; Wageningen University, Sub-Department of Environmental Technology, 6700 AA Wageningen, The Netherlands; orcid.org/0000-0001-6832-3218; Phone: +41 61 228 5686; Email: Markus.Lenz@fhnw.ch

Authors

Sebastian Hedwig – FHNW, Institute for Ecopreneurship, 4132 Muttentz, Switzerland; Department of Chemistry, University of Basel, 4058 Basel, Switzerland; orcid.org/0000-0002-7061-3596

Bengi Yagmurlu – Department of Process Metallurgy and Metal Recycling, RWTH Aachen University, 52056 Aachen, Germany; MEAB Chemie Technik GmbH, 52068 Aachen, Germany

Danyu Huang – State Key Laboratory of Pollution Control and Resource Reuse, School of the Environment, Nanjing University, Nanjing 210023 Jiangsu Province, P. R. China

Oliver von Arx – Department of Chemistry, University of Basel, 4058 Basel, Switzerland

Carsten Dittrich – MEAB Chemie Technik GmbH, 52068 Aachen, Germany

Edwin C. Constable – Department of Chemistry, University of Basel, 4058 Basel, Switzerland

Bernd Friedrich – Department of Process Metallurgy and Metal Recycling, RWTH Aachen University, 52056 Aachen, Germany

Complete contact information is available at:

<https://pubs.acs.org/doi/10.1021/acssuschemeng.2c01056>

Author Contributions

[†]S.H. and B.Y. contributed equally to this paper.

Notes

The authors declare no competing financial interest.

■ ACKNOWLEDGMENTS

This project has received funding from the European Union's Horizon 2020 Research and Innovation Programme under grant agreement No. 730105 (SCALE: www.scale-project.eu/). This work was supported by the Swiss State Secretariat for Education, Research and Innovation (SERI) under contract number 16.0155. The opinions expressed and arguments employed herein do not necessarily reflect the official views of the Swiss Government. Roman Schäfer and Kirsten Remmen are kindly thanked for their assistance during this study.

■ REFERENCES

- (1) Ahmad, Z. The properties and application of scandium-reinforced aluminum. *JOM* **2003**, *35*, 35–39.
- (2) Botelho Junior, A. B.; Espinosa, D.; Vaughan, J.; Tenório, J. Recovery of scandium from various sources: A critical review of the state of the art and future prospects. *Miner. Eng.* **2021**, *172*, No. 107148.
- (3) Remmen, K.; Schäfer, R.; Hedwig, S.; Wintgens, T.; Wessling, M.; Lenz, M. Layer-by-layer membrane modification allows scandium recovery by nanofiltration. *Environ. Sci.: Water Res. Technol.* **2019**, *5*, 1683–1688.
- (4) Gambogi, J. *USGS Mineral Commodity Summary: Scandium*, 2022.
- (5) European Commission. *On the 2017 list of Critical Raw Materials for the EU: COM(2017) 490 final*, 2017.
- (6) European Commission. *Critical Raw Materials Resilience: Charting a Path towards Greater Security and Sustainability: COM/2020/474 Final*, 2020.
- (7) Wang, W.; Pranolo, Y.; Cheng, C. Y. Metallurgical processes for scandium recovery from various resources: A review. *Hydrometallurgy* **2011**, *108*, 100–108.
- (8) Alkan, G.; Yagmurlu, B.; Cakmakoglu, S.; Hertel, T.; Kaya, S.; Gronen, L.; Stopic, S.; Friedrich, B. Novel Approach for Enhanced Scandium and Titanium Leaching Efficiency from Bauxite Residue with Suppressed Silica Gel Formation. *Sci. Rep.* **2018**, *8*, No. 5676.
- (9) Kaya, S.; Dittrich, C.; Stopic, S.; Friedrich, B. Concentration and Separation of Scandium from Ni Laterite Ore Processing Streams. *Metals* **2017**, *7*, No. 557.
- (10) Gambogi, J. *USGS Minerals Information: Titanium and Titanium Dioxide*, 2021.
- (11) Zhang, W.; Zhu, Z.; Cheng, C. Y. A literature review of titanium metallurgical processes. *Hydrometallurgy* **2011**, *108*, 177–188.
- (12) Perks, C.; Mudd, G. Titanium, zirconium resources and production: A state of the art literature review. *Ore Geol. Rev.* **2019**, *107*, 629–646.
- (13) Gázquez, M. J.; Bolívar, J. P.; Garcia-Tenorio, R.; Vaca, F. A Review of the Production Cycle of Titanium Dioxide Pigment. *Mater. Sci. Appl.* **2014**, *05*, 441–458.
- (14) Yagmurlu, B.; Orberger, B.; Dittrich, C.; Croisé, G.; Scharfenberg, R.; Balomenos, E.; Panias, D.; Mikeli, E.; Maier, C.; Schneider, R.; Friedrich, B.; Dräger, P.; Baumgärtner, F.; Schmitz, M.; Letmathe, P.; Sakkas, K.; Georgopoulos, C.; van den Laan, H. *Sustainable Supply of Scandium for the EU Industries from Liquid Iron Chloride Based TiO₂ Plants*, International Conference on Raw Materials and Circular Economy, 2021.
- (15) Zhou, J.; Ning, S.; Meng, J.; Zhang, S.; Zhang, W.; Wang, S.; Chen, Y.; Wang, X.; Wei, Y. Purification of scandium from concentrate generated from titanium pigments production waste. *J. Rare Earths* **2020**, *39*, 194–200.
- (16) Qiu, H.; Wang, M.; Xie, Y.; Song, J.; Huang, T.; Li, X.-M.; He, T. From trace to pure: Recovery of scandium from the waste acid of titanium pigment production by solvent extraction. *Process Saf. Environ. Prot.* **2019**, *121*, 118–124.
- (17) Zou, D.; Li, H.; Chen, J.; Li, D. Recovery of scandium from spent sulfuric acid solution in titanium dioxide production using synergistic solvent extraction with D2EHPA and primary amine N1923. *Hydrometallurgy* **2020**, *197*, No. 105463.
- (18) Salman, A. D.; Juzsakova, T.; Mohsen, S.; Abdullah, T. A.; Le, P.-C.; Sebestyen, V.; Sluser, B.; Cretescu, I. Scandium Recovery Methods from Mining, Metallurgical Extractive Industries, and Industrial Wastes. *Materials* **2022**, *15*, No. 2376.
- (19) Zhou, J.; Ma, S.; Chen, Y.; Ning, S.; Wei, Y.; Fujita, T. Recovery of scandium from red mud by leaching with titanium white waste acid and solvent extraction with P204. *Hydrometallurgy* **2021**, *204*, No. 105724.
- (20) Zhou, J.; Yu, Q.; Huang, Y.; Meng, J.; Chen, Y.; Ning, S.; Wang, X.; Wei, Y.; Yin, X.; Liang, J. Recovery of scandium from white waste acid generated from the titanium sulphate process using solvent extraction with TRPO. *Hydrometallurgy* **2020**, *195*, No. 105398.
- (21) Smirnov, A. L.; Titova, S. M.; Rychkov, V. N.; Bunkov, G. M.; Semenishchev, V. S.; Kirillov, E. V.; Poponin, N. N.; Svirsky, I. A. Study of scandium and thorium sorption from uranium leach liquors. *J. Radioanal. Nucl. Chem.* **2017**, *312*, 277–283.
- (22) Yagmurlu, B.; Alkan, G.; Kakalashe, B.; Schier, C.; Gronen, L.; Koiba, I.; Dittrich, C.; Friedrich, B. Synthesis of Scandium Phosphate after Peroxide Assisted Leaching of Iron Depleted Bauxite Residue (Red Mud) Slags. *Sci. Rep.* **2019**, *9*, No. 11803.
- (23) Yagmurlu, B.; Dittrich, C.; Friedrich, B. Precipitation Trends of Scandium in Synthetic Red Mud Solutions with Different Precipitation Agents. *J. Sustainable Metall.* **2017**, *3*, 90–98.
- (24) European Commission. *Reference Document on Best Available Techniques for the Manufacture of Large Volume Inorganic Chemicals - Solids and Others Industry*, Seville: Spain, 2007.
- (25) Rene, E. R. *Sustainable Heavy Metal Remediation: Volume 1: Principles and Processes*, Springer International Publishing: Cham, 2017; pp. 101–120.
- (26) García, A. C.; Latifi, M.; Amini, A.; Chaouki, J. Separation of Radioactive Elements from Rare Earth Element-Bearing Minerals. *Metals* **2020**, *10*, No. 1524.
- (27) Svandova, M.; Raschman, P.; Sucik, G.; Dorakova, A.; Fedorockova, A. Removal of Heavy Metals From Wastewater Using Caustic Calcinated Magnesia. *Acta Metall. Slovaca* **2015**, *21*, 247–252.
- (28) Blais, J. F.; Djedidi, Z.; Cheikh, R. B.; Tyagi, R. D.; Mercier, G. Metals Precipitation from Effluents: Review. *Pract. Period. Hazard. Toxic Radioact. Waste Manage.* **2008**, *12*, 135–149.
- (29) Yagmurlu, B.; Dittrich, C.; Friedrich, B. Effect of Aqueous Media on the Recovery of Scandium by Selective Precipitation. *Metals* **2018**, *8*, 314.
- (30) Kose Mutlu, B.; Cantoni, B.; Turolla, A.; Antonelli, M.; Hsu-Kim, H.; Wiesner, M. R. Application of nanofiltration for Rare Earth Elements recovery from coal fly ash leachate: Performance and cost evaluation. *Chem. Eng. J.* **2018**, *349*, 309–317.
- (31) Schütte, T.; Niewersch, C.; Wintgens, T.; Yüce, S. Phosphorus recovery from sewage sludge by nanofiltration in diafiltration mode. *J. Membr. Sci.* **2015**, *480*, 74–82.
- (32) Hussain, Y. A.; Al-Saleh, M. H.; Ar-Ratrou, S. S. The effect of active layer non-uniformity on the flux and compaction of TFC membranes. *Desalination* **2013**, *328*, 17–23.
- (33) Wanner Engineering, Inc. G03 Series Datasheet, 2021, <https://www.hydra-cell.com/ltr2/access.php?file=pdf/G03-Datasheet.pdf>.
- (34) Mdemagh, Y.; Hafiane, A.; Ferjani, E. Characterization and modeling of the polarization phenomenon to describe salt rejection by nanofiltration. *Appl. Polym. Symp.* **2018**, *1*, No. 5.
- (35) Lei, Q.; He, D.; Zhou, K.; Zhang, X.; Peng, C.; Chen, W. Separation and recovery of scandium and titanium from red mud leaching liquor through a neutralization precipitation-acid leaching approach. *J. Rare Earths* **2021**, *39*, 1126–1132.
- (36) Hung, N. T.; Le Thuan, B.; Thanh, T. C.; Watanabe, M.; van Khoai, D.; Thuy, N. T.; Nhuan, H.; Minh, P. Q.; Mai, T. H.; van Tung, N.; Tra, D. T. T.; Jha, M. K.; Lee, J.-Y.; Jyothi, R. K. Separation of thorium and uranium from xenotime leach solutions by solvent extraction using primary and tertiary amines. *Hydrometallurgy* **2020**, *198*, No. 105506.


- (37) Gupta, B.; Deep, A.; Malik, P.; Tandon, S. N. Extraction and Separation of Some 3d Transition Metal Ions Using Cyanex 923. *Solvent Extr. Ion Exch.* **2002**, *20*, 81–96.
- (38) Yurtov, E. V.; Murashova, N. M. Gels, emulsions, and liquid crystals in extraction systems with Di(2-ethylhexyl)phosphoric acid. *Theor. Found Chem. Eng.* **2007**, *41*, 737–742.
- (39) Chen, Y.; Ma, S.; Ning, S.; Zhong, Y.; Wang, X.; Fujita, T.; Wei, Y. Highly efficient recovery and purification of scandium from the waste sulfuric acid solution from titanium dioxide production by solvent extraction. *J. Environ. Chem. Eng.* **2021**, *9*, No. 106226.
- (40) Yagmurlu, B.; Dittrich, C.; Friedrich, B. *Innovative Scandium Refining Processes from Secondary Raw Materials*, European Scandium Inventory Workshops2018.
- (41) Yagmurlu, B.; Dittrich, C.; Davris, P.; Balomenos, E.; Pilichou, A.; Panias, D.; Friedrich, B. *Recovery of Scandium from Bauxite Residue Via Solvent Extraction*, Proceedings of 3rd International Bauxite Residue Valorisation and Best Practices Conference, 2020.
- (42) Wang, W.; Cheng, C. Y. Separation and purification of scandium by solvent extraction and related technologies: a review. *J. Chem. Technol. Biotechnol.* **2011**, *86*, 1237–1246.
- (43) Wang, W.; Pranolo, Y.; Cheng, C. Y. Recovery of scandium from synthetic red mud leach solutions by solvent extraction with D2EHPA. *Sep. Purif. Technol.* **2013**, *108*, 96–102.
- (44) Wang, D.; Li, Y.; Wu, J.; Xu, G. Mechanism of the extractant loss in lanthanide extraction process with saponified organophosphorus acid extraction systems - II: formation of aqueous aggregates: Mechanism of the extractant loss in lanthanide extraction process with saponified organophosphorus acid extraction systems - II: formation of aqueous aggregates. *Solvent Extr. Ion Exch.* **1996**, *14*, 585–601.
- (45) Sun, M.; Liu, S.; Zhang, Y.; Liu, M.; Yi, X.; Hu, J. Insights into the saponification process of di(2-ethylhexyl) phosphoric acid extractant: Thermodynamics and structural aspects. *J. Mol. Liq.* **2019**, *280*, 252–258.
- (46) Kaya, Ş.; Peters, E.; Forsberg, K.; Dittrich, C.; Stopic, S.; Friedrich, B. Scandium Recovery from an Ammonium Fluoride Strip Liquor by Anti-Solvent Crystallization. *Metals* **2018**, *8*, No. 767.
- (47) Li, K.; Fan, Q.; Chuai, H.; Liu, H.; Zhang, S.; Ma, X. Revisiting Chlor-Alkali Electrolyzers: from Materials to Devices. *Trans. Tianjin Univ.* **2021**, *27*, 202–216.



ACS
BIO & MED
AN OPEN ACCESS JOURNAL OF
THE AMERICAN CHEMICAL SOCIETY
CHEM
Au

Editor-in-Chief: **Prof. Shelley D. Minteer**, University of Utah, USA

Deputy Editor
Prof. Squire J. Booker
Pennsylvania State University, USA

Open for Submissions 

pubs.acs.org/blomedchemau  **ACS Publications**
Most Trusted. Most Cited. Most Read.